J Biol Phys (2014) 40:387–400
DOI 10.1007/s10867-014-9357-9

ORIGINAL PAPER

Assembly and stability of *Salmonella enterica* ser. Typhi TolC protein in POPE and DMPE

Siew Wen Leong · Theam Soon Lim · Gee Jun Tye · Asma Ismail · Ismail Aziah · Yee Siew Choong

Received: 24 March 2014 / Accepted: 23 May 2014 / Published online: 11 July 2014

Abstract In this work we assessed the suitability of two different lipid membranes for the simulation of a TolC protein from *Salmonella enterica* serovar Typhi. The TolC protein family is found in many pathogenic Gram-negative bacteria including *Vibrio cholera* and *Pseudomonas aeruginosa* and acts as an outer membrane channel for expulsion of drug and toxin from the cell. In *S. typhi*, the causative agent for typhoid fever, the TolC outer membrane protein is an antigen for the pathogen. The lipid environment is an important modulator of membrane protein structure and function. We evaluated the conformation of the TolC protein in the presence of DMPE and POPE bilayers using molecular dynamics simulation. The *S. typhi* TolC protein exhibited similar conformational dynamics to TolC and its homologues. Conformational flexibility of the protein is seen in the C-terminal, extracellular loops, and α-helical region. Despite differences in the two lipids, significant similarities in the motion of the protein in POPE and DMPE were observed, including the rotational motion of the C-terminal residues and the partially open extracellular loops. However, analysis of the trajectories demonstrated effects of hydrophobic matching of the TolC protein in the membrane, particularly in the lengthening of the lipids and subtle movements of the protein's β-barrel towards the lower leaflet in DMPE. The study exhibited the use of molecular dynamics simulation in revealing the differential effect of membrane proteins and lipids on each other. In this study, POPE is potentially a more suitable model for future simulation of the *S. typhi* TolC protein.

Keywords *Salmonella typhi* · TolC protein · Molecular dynamics simulation · POPE · DMPE

S. W. Leong · T. S. Lim · G. J. Tye · Y. S. Choong (✉)
Institute for Research in Molecular Medicine, Universiti Sains Malaysia, 11800 Minden, Pulau Pinang, Malaysia
e-mail: yeesiew@usm.my

A. Ismail · I. Aziah
Institute for Research in Molecular Medicine, Kampus Kesihatan, Universiti Sains Malaysia, 16150 Kubang Kerian, Kelantan, Malaysia

1 Introduction

Typhoid fever is a febrile enteric disease caused by the pathogen *Salmonella enterica* ser. Typhi. The pathogen is restricted to human host and causes fever, malaise, headache, diarrhea or constipation, and in extreme cases ileocecal perforations and intestinal hemorrhages [1]. A study conducted by Crump and colleagues estimated that the disease infects 21.7 million patients and kills 200,000 annually [2]. An outer membrane protein (OMP) was demonstrated to be antigenic for *S. typhi* and subsequently developed into TYPHIDOT (Reszon Diagnostics International, Subang Jaya, Selangor, Malaysia), a rapid dot enzyme immunoassay test for typhoid fever [3, 4]. The protein was shown to be a homologue of *Escherichia coli* TolC efflux pump through comparative modeling [5]. TolC and its homologues, including *Vibrio cholerae* VceC [6] and *Pseudomonas aeruginosa* OprM [7], form tripartite pumps that are involved in the type I secretion system, exporting enzymes, toxins, small noxious agents, heavy metals and antibiotics from the cell [8], thus contributing to multidrug resistance in a number of Gram-negative bacteria pathogens. TolC functions as a passage for the solute from the cytoplasm to the external medium. The transport process is driven by an inner membrane transporter connected to the TolC exit duct via an inner-membrane linked periplasmic adaptor protein. In *E. coli*, TolC has been shown to form a proton motive force-dependent efflux pump with AcrAB. AcrA is a periplasmic lipoprotein that forms a complex with AcrB, a proton-substrate antiporter [9] and recruits TolC to assemble the tripartite efflux pump [10]. Besides AcrAB, TolC can also be recruited by other transporter systems, namely AcrEF [11], YhiUV [12], EmrAB [13] and its homolog EmrKY [14], MdtABC [15], and the MacAB macrolide extrusion system [16].

In recent decades, computational modeling and simulation has emerged as a widely used tool to investigate the structural and dynamical properties of membrane proteins. This is due to many difficulties in studying the proteins in vivo or in vitro because of the problem involving crystallization of the proteins. MD techniques, in particular, have been employed to model structures of proteins in equilibrium [17], transport processes [18], opening and closing of gating channels [19], and also self-assembly of lipids around membrane proteins [20].

Many studies are also concerned with the effects of membrane and membrane proteins on each other, including experimental and computational approaches. Since a large percentage of the protein surface is in contact with the membrane lipids, the membrane plays an important role in modulating the protein structure and function. Interaction between membrane proteins and their surrounding membrane components is often critical to their folding and stability. Several experimental and theoretical studies have also demonstrated that subtle differences in membrane properties such as thickness, order, and composition, influence the membrane protein structure [21]. For example, it is known that membrane thickness negatively influences the gramicidin channel lifetime [22] and may induce opening and closing of mechanosensitive channels [23, 24]. In turn, insertion of proteins into the membrane also significantly affects membrane structures, in particular peripheral lipids that are in close contact with the proteins [25–27, 21].

Therefore, it is imperative that appropriate lipid models are employed to simulate membrane proteins in a membranous environment. In most membrane protein simulation studies, the lipid model is chosen arbitrarily and usually phosphatidylcholine (PC) lipids such as DPPC, DLPC, DMPC, or POPC are chosen. Phosphatidylcholine lipids are one of the most abundant lipids in nature, and make up the major component in eukaryotic cells [28]. PC lipids are well studied both in simulations and experimentally [29], which facilitates comparison between simulation and prior works. The availability of a force-field parameter can also influence the choice of lipid model employed in the simulation study. However, we feel that a more methodical approach to selecting the membrane component of a membrane protein simulation would be advisable.

Here, molecular dynamics (MD) simulation was used to infer the effect of different lipid bilayers on the structure of the *Salmonella enterica* ser. Typhi TolC protein. The TolC protein was modeled in two different membrane bilayers, namely 1-palmitoyl-2-oleoyl-*sn*-glycero-3-phosphoethanolamine (POPE) (Fig. 1a) and 1,2-dimyristoyl-*sn*-glycero-3-phosphoethanolamine (DMPE) (Fig. 1b). Phosphatidylethanolamine (PE) lipids were considered as these constitute the major lipid species in *E. coli* outer membrane [30, 31].

Results showed that effects of hydrophobic matching can be observed from the simulation of the TolC protein in DMPE, although the protein remained reasonably stable in both lipids. For longer simulations, embedding the protein in POPE will reduce the chances of the protein structure being influenced by effects of hydrophobic matching. Therefore, the study also highlights the risk of arbitrarily using any membrane component for MD simulation of proteins in the membrane. Employing a the membrane component that is unsuitable for the protein's hydrophobic area may induce conformational changes that may affect structural analysis of the protein.

2 Methodology

2.1 Simulation setup

A comparative model of the *S. typhi* TolC protein [5] was used as the starting structure in this study. Polar hydrogens were added using the program Reduce [32]. Then, cavity waters were added with the program Dowser [33]. This was followed by solvation of the protein with Helmut Grubmuller's Solvate to fill the protein pore and create a water shell around the protein. The starting structure for the POPE membrane is a CHARMM36 pre-equilibrated patch of 80 lipids were obtained from http://terpconnect.umd.edu/~jbklauda/research/download.html (accessed 22/2/2012). Meanwhile, a small membrane patch of 80 DMPE lipids was generated with the CHARMM-GUI membrane builder [34] as pre-equilibrated DMPE is not available. Both membrane models were enlarged to 180×180 $Å^2$ using the GROMACS program *genbox*. The solvated protein was consequently embedded in the membrane patches by aligning the mass center of the β-barrel with the mass center of the membrane patch in VMD. Overlapping lipids and water molecules were specified as those within 0.8 Å from any protein atoms and were deleted with VMD atom selection function (www.ks.uiuc.edu/Training/Tutorials/science/membrane/mem-tutorial.pdf). The system was then fully solvated in a water box by the GROMACS program genbox. Water molecules added at the membrane hydrophobic lipid tails were also deleted. Finally, the system was neutralized and ionized to a concentration of 0.1 M KCl with the GROMACS program *genion*. In the simulation with POPE, the final system consists of 857 lipids, 132,520 water molecules, and 729 counterions, totaling 526,753 atoms. Meanwhile, in the simulation with DMPE, the system is made up of 850 lipids, 137,837 water molecules, and 841 counterions, totaling 528,341 atoms.

2.2 Simulation conditions

All simulations were performed with GROMACS version 4.5.4 [35]. The protein and the lipids were treated with CHARMM22/CMAP [36, 37] and the CHARMM36 parameter [38], respectively. TIP3P was used to model the water. The steepest descent energy minimization was performed until the forces in the system were <1,000 kJ/mol/nm. 3D periodic boundary

condition was imposed on all simulations. A 200-ps NVT run with modified Berendsen thermostat [39] were then imposed on both runs, equilibrating the temperature to the system with POPE and DMPE to 310.15 and 323 K, respectively. It was necessary to perform simulations at different temperatures as these are the phase transition temperatures for POPE and DMPE, respectively, at their biologically relevant liquid crystal phase. Restraints were imposed on protein and lipid phosphate atoms during the equilibration. Following the temperature equilibration, a 1-ns NPT run was performed to equilibrate the pressure semi-isotropically at 1 atm with the Parrinello–Rahman method [40]. Restraints on lipid phosphate atoms were relaxed and temperature coupling was controlled with Nose–Hoover method [41, 42]. Finally, production runs with the protein released were performed for 5 ns. In all equilibrations and production simulations, long-range electrostatics was treated with PME. A switch function was used to evaluate the Lennard–Jones potential from 8 to 12 Å. Real-space sums were cut off at 12 Å. The LINCS algorithm was used to constrain bond lengths [43] and to allow a timestep of 2 fs during the simulation. MD simulations were performed on a cluster of eight Intel Xeon X3360 2.8-GHz processors. This translates into average performance of 179.7 ns/h and 169.5 ns/h simulation for the DMPE and POPE systems, respectively.

3 Results

3.1 Stability of membrane lipids in simulation

In any membrane protein simulation it is necessary to determine whether the membrane component is in the required liquid crystalline phase. Therefore, in silico lipid simulations were usually assessed on the reproducibility of several experimental parameters, namely the area per lipid (APL), membrane thickness, and tail order parameter. Area per lipid (APL) was calculated using a combined Voronoi tessellation and Monte Carlo integration method [44]. Figure 2a shows the time evolution of the APL of both simulations. In the initial 2 ns of simulation, the APL decreases steadily, possibly indicating that the lipid molecules are still equilibrating around the protein. APL calculated from the simulation with POPE was 58.0± 0.5 $Å^2$ after 3 ns. The figure is consistent with prior simulations studies that recorded APL between 56.3 and 59.2 $Å^2$ [45, 38] and also experimentally determined the value of 56.6 $Å^2$

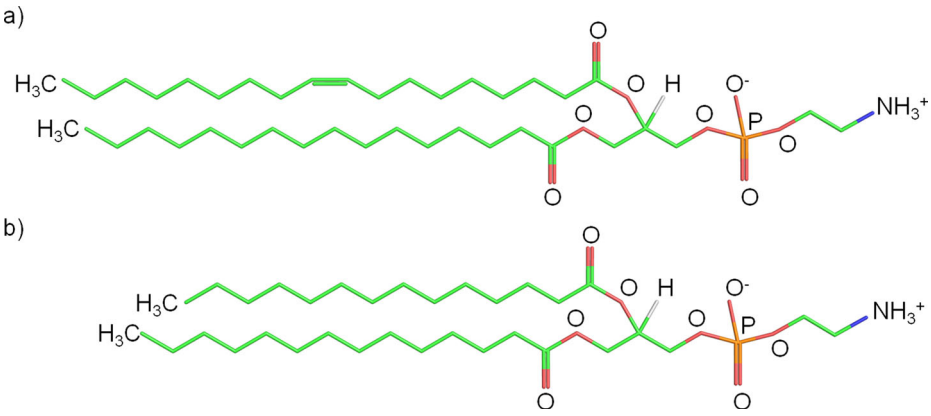

Fig. 1 2D molecular structure of POPE (**a**) and DMPE (**b**)

[46]. In the simulation with DMPE, APL was 53.5±0.3 Å^2 after 3 ns, reflecting the experimental APL of 53.7 Å^2 [47].

The thickness of the membrane was estimated from the density of lipid phosphate atoms along the *z*-axis. The difference between the peaks in the density graph corresponds to the membrane thickness. POPE thickness, averaged over the last 2 ns of the simulation, was 43.5 Å, which was comparable to the experimental thickness of 41.8 Å [46]. Meanwhile, the calculated DMPE thickness was 42.6 Å, depicting a thicker membrane when compared to the thickness of DMPE obtained experimentally (37.6 Å–40.4) [46, 47].

The deuterium order parameter can be calculated from

$$-S_{CD} = \left\langle \frac{(3\cos^2\theta)-1}{2} \right\rangle$$

where θ refers to the angle between the C-D bond and the membrane normal, and the brackets indicate that the values were averaged over all equivalent atoms over time. The order parameter profile (Fig. 2b) was similar to the experimentally determined order, including the dip in value for carbon 9 and 10 for the POPE sn-2 chain. Overall, the membrane simulations were consistent with available experimental data of the respective lipids in liquid crystal phase as shown above.

3.2 Structural stability of the *S. typhi* TolC protein

Conformational stability of the TolC protein in POPE and DMPE was measured by calculating the root mean square deviation (RMSD), root mean square fluctuation (RMSF), and time evolution of the secondary structure during the simulation. The RMSD was calculated with respect to the initial structure as a function of time and shows the extent of structural flexibility. The RMSD profile showed that most regions of the TolC protein in POPE remained relatively stable throughout the simulations (Fig. 3a). The extracellular loops and periplasmic domains have larger deviations from the starting structure. The extracellular loops of RMSD fluctuated around 2.5–3.0 Å after a 1-ns simulation. The periplasmic domain showed much higher fluctuations (~5.5 Å). The TolC protein in both POPE and DMPE showed a similar RMSD profile, as demonstrated in the TM region, which deviate approximately 1 Å from the starting structure (Fig. 3a). The extracellular loops in DMPE showed more mobility than in POPE. We notice the occurrence of higher RMSD in the periplasmic domain compared to prior simulation of similar channels, as the model incorporated the flexible C-terminal 43 residues that were truncated in *E. coli* TolC crystallization [8, 48]. The RMSF plot reaffirmed the observation from RMSD analysis (Fig. 3b). The protein RMSF profile was similar in both POPE and DMPE. Peaks on the plot corresponded to flexible regions on the protein, i.e., the extracellular loops (residue 734–737, 1205–1207), equatorial domain (residue 199–204, 1140) and C-terminal (residue 424–467, 891–934, 1359–1401). While residues on the extracellular loops and equatorial domain fluctuated at more than 2 Å, some residues on the coils of C-terminal have RMSF values exceeding 10 Å, showing great flexibility. Nevertheless, the protein conformation was well preserved in both environments, evidenced from the time evolution of the protein secondary structure elements (Fig. 4).

The conformational dynamics of the protein was further assessed by principal component analysis (PCA). PCA of the trajectory in POPE simulation showed that the first 13 eigenvectors account for 90% of the total motion in the system. From this, the first eigenvector was responsible for 49% of the dynamics, whereas the second eigenvector contributed a

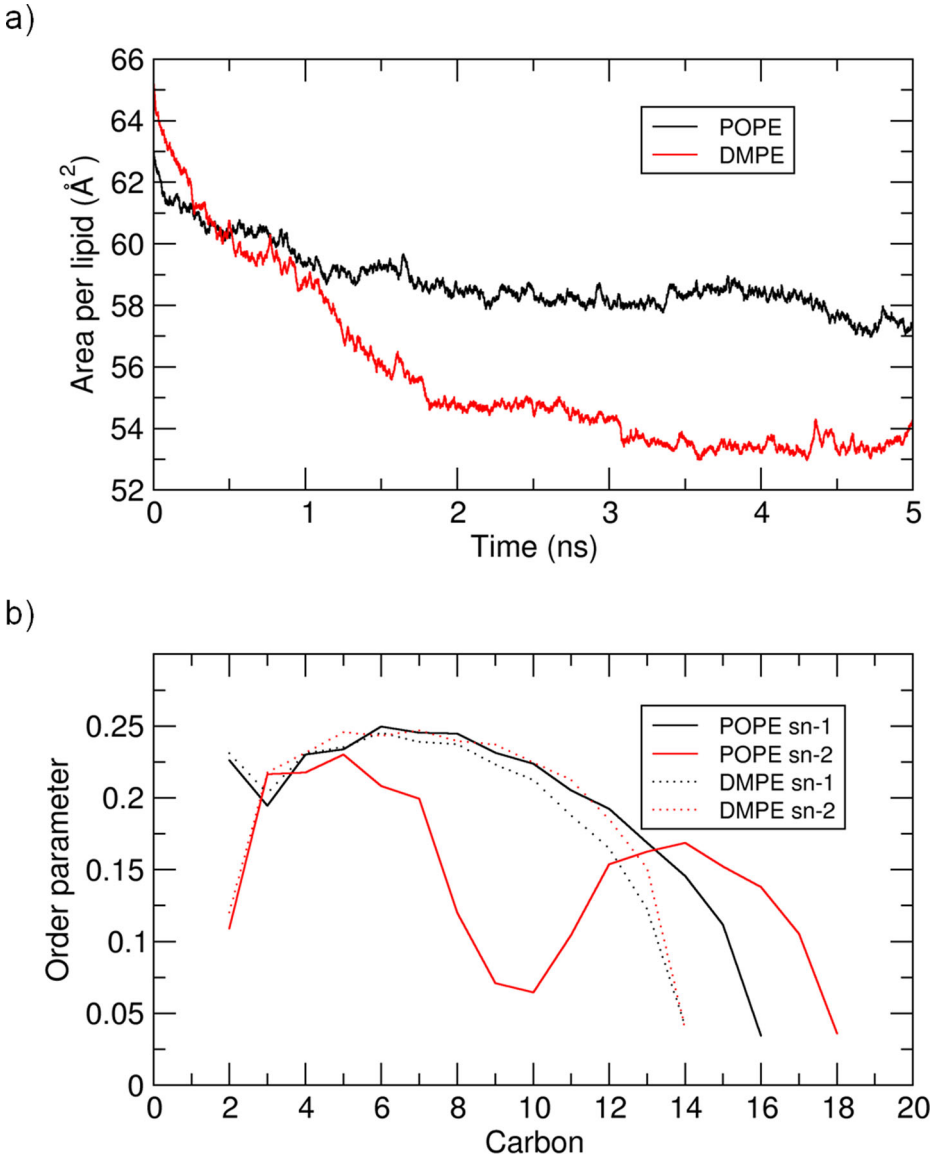

Fig. 2 Stability of membrane models. **a** Time evolution of area per lipid of POPE and DMPE. **b** Deuterium order parameter of POPE and DMPE lipids

further 17%. In the DMPE simulation, the first 15 eigenvectors were responsible for 89% of the fluctuations. The largest motions can be attributed to the first and second eigenvector, which accounted for 27% and 25% of the total motion, respectively. The third eigenvector described a further 16% of the protein motion.

A porcupine plot was generated linking each C_α atom with an arrow that points to the direction of the associated eigenvector to visualize the modes of motion from the PCA (Figs. 4b, 5a). The length of the arrow is proportional to the amplitude of the motion. The

largest amplitude of motions revealed by PCA also occurred in the C-terminal domain and extracellular loops similar to the RMSD plot (Fig. 3).

PCA revealed that general motion of the protein in both lipids are similar, including the floppy up and down and twirling of the C-terminal residues around the main channel (Fig. 5b). However, it is also evident that in DMPE lipids, starting from the top of extracellular loops, the β-barrel region seemed to move towards the lower leaflet. This movement could possibly be an adaptation of the barrel to the bilayer.

4 Discussion

With progress in computational power, most recent simulations were performed at an extended time length (~100 ns) with the microsecond range already being attainable. Extended simulation is not only commendable but may even be a necessity as lipids take a longer time to properly equilibrate among themselves and around the protein as compared to the typical protein in water simulation. Biological membrane phenomena, such as lateral diffusion of lipids, occur over tens of nanoseconds [49]. In recent simulation studies of membrane lipids and membrane proteins in lipid bilayers, 20 ns or more of the simulation time are discarded as the equilibration period [50, 51]. While the use of a randomly chosen lipid model in a simulation study may be too arbitrary, it is also impossible to perform simulations of all available lipid models to determine a good model for any membrane protein simulation. Therefore, we have simulated and assessed the stability of *S. typhi* TolC protein in POPE and DMPE lipids to determine the suitability of both lipid models for future simulations of the protein. Phosphatidylethanolamine lipids are the most dominant lipid species in the outer membrane of *E. coli* [30, 31] and so would be a good mimic for the Gram-negative bacteria membrane environment.

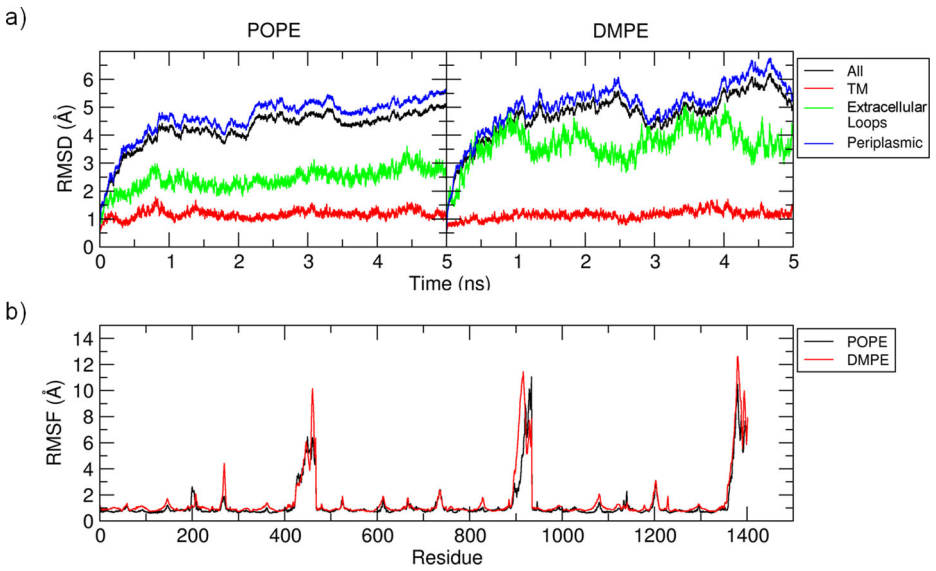

Fig. 3 Structural stability of the *S. typhi* TolC protein. **a** Protein Cα atom RMSD of the protein in POPE and DMPE. **b** RMSF of the TolC protein

Simulation analysis indicated that the TolC protein exhibits flexibility in the C-terminal residues and extracellular loop regions. The occurrence of higher RMSD in the periplasmic domain compared to prior simulation of similar channels is to be expected, as the model incorporated the flexible C-terminal 43 residues that were truncated in TolC crystallization [8, 48]. Whereas in the extracellular loops in DMPE, the higher flexibility can be explained as the loops were more exposed and relieved from interacting with the lipid head groups due to the thinner environment.

PCA was performed on backbone atoms of both trajectories to identify slow, concerted motions of the protein conformations. This technique can be used to decompose the motions of a protein into a few principal components characterized by an eigenvector and eigenvalue. Principal components with the highest eigenvalues usually represent the slowest protein motions, which bring about the largest and most significant conformational changes. PCA analysis revealed that most motions occurred in the C-terminal 43 residues, extracellular loops and the lower part of the helices of the periplasmic domain. This echoes the findings of prior simulations of TolC whereby the surface exposed loops and the tip of α-helices are shown to be most flexible [48]. From the PCA data, we observed the collapsing movement of one or two extracellular loops with the opening of another. TolC simulation by Raunest and Kandt (2012) also showed that partially open extracellular loops seem to be the preferred conformation [17]. Therefore, we believe that the partially opened loops may be the preferred conformation in the absence of other protein components of the efflux pump like AcrA and AcrB.

Effects of hydrophobic matching were observed by the TolC protein in DMPE. Hydrophobic mismatch occurs when the hydrophobic environment of lipid tails is unable to fully accommodate the protein, resulting in adaptation of both the lipid and the protein in order

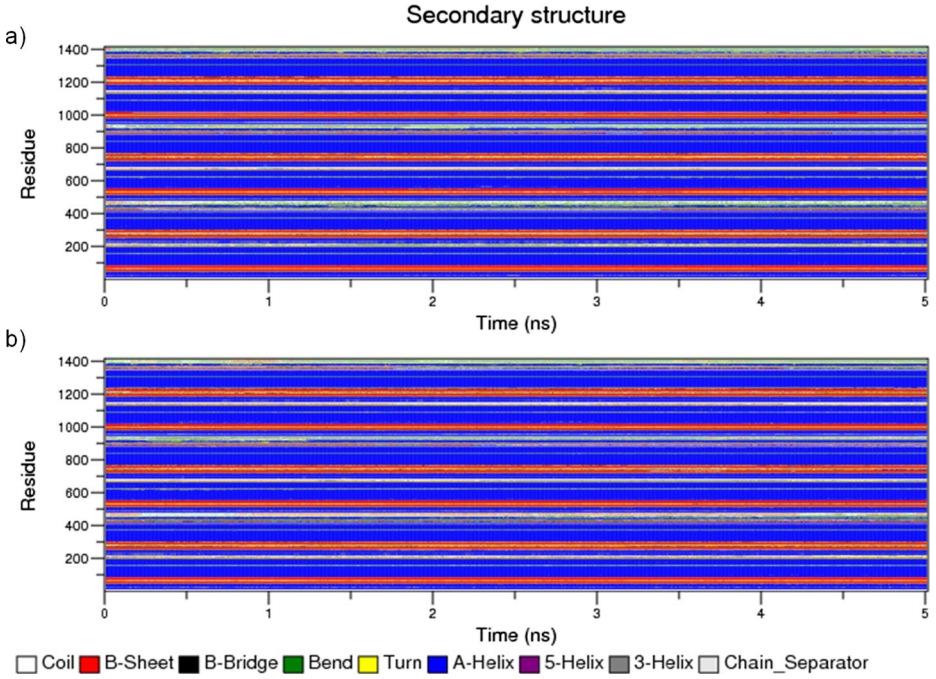

Fig. 4 Time evolution of the protein secondary structure in POPE (**a**) and DMPE (**b**)

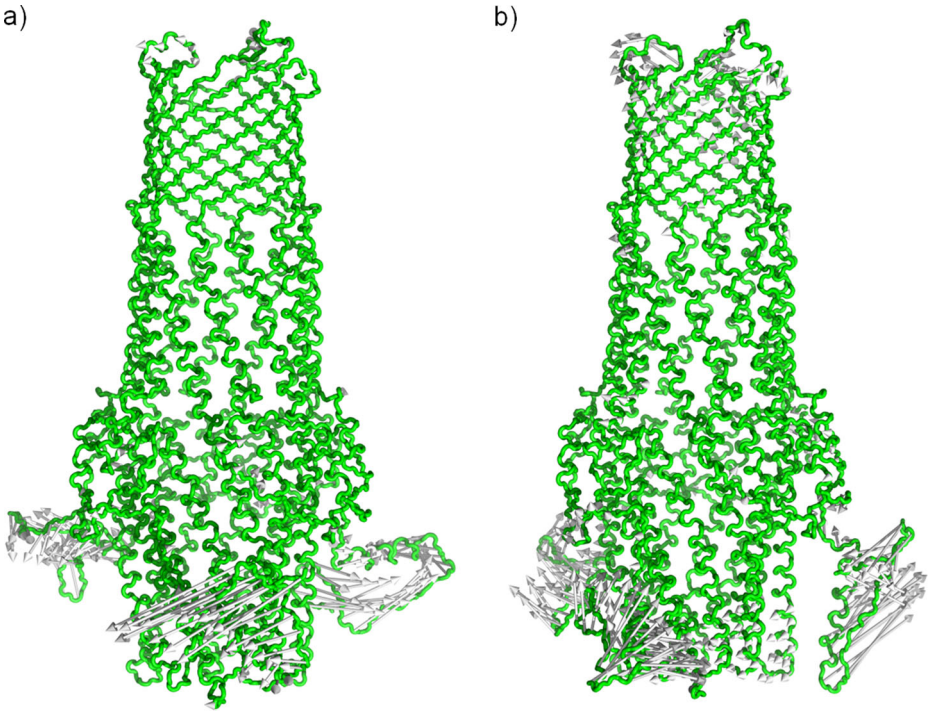

Fig. 5 Porcupine plot depicting the direction and magnitude of movement of the first eigenvector in POPE (**a**) and DMPE (**b**)

to minimize the energetic consequences of exposure of the protein hydrophobic residues to the solvent [52]. While the lipid environment is a strong modulator for protein structure and function, β-barrels/β-helical proteins also appear to be more rigid and impose a greater restraint on lipid packing compared to an α-helical bundle [53]. This was evident from the remarkable stability of the β-barrel region in both bilayers, registering an RMSD of ~1 Å. However, in response to the thinner environment, structural rearrangement was demonstrated by the movement of the barrel region towards the lower lipid leaflet. The *E. coli* mechanosensitive channel was demonstrated to exhibit comparable rearrangements in response to hydrophobic mismatch in a simulation study [23]. The higher thickness of the DMPE lipids compared to the experimentally determined value may also be a form of adaptation of the lipids to the TolC protein β-barrel. The DMPE membrane presented a thinner hydrophobic environment than POPE and allowed the lipid tails to extend in order to fully adapt to the TolC protein hydrophobic region. Simulation studies of KALP and WALP model transmembrane peptides in lipid bilayers estimated that insertion of the protein induces ~1 Å changes in the lipid thickness in most cases and up to a difference 3 Å in extreme situations [54, 55].

The present work serves as an explorative study to determine the differential effect of the TolC protein and lipid membrane on each other. Most atomistic membrane protein simulations employ pure, one-component lipid bilayers, while some report simulations using mixed bilayers, typically a mixture of two lipids [56]. A mixture of the lipids may be incorporated to build a membrane model to provide a resemblance to a mix of lipids in natural membranes. When using mixed bilayers, the simulation period must be extended to allow lipids of different species to equilibrate to each other and to the membrane protein. Recently, new parameters

have been developed for other major membrane components including lipopolysaccharides, glycerol, and peptidoglycans, allowing more realistic simulations of the membrane protein and its environment. With the progress in modeling bacterial lipopolysaccharides (LPS) [57], more accurate representation of the Gram-negative bacteria outer membrane can be modeled [58]. However, LPS molecules can have diverse structure and composition [59]. A single cell can modify its LPS composition in response to conditions in its environment, which makes it difficult to model LPS molecules for all organisms.

In addition, the use of united atom and coarse grain force fields is increasingly popular. It reduces the complexity of lipid model representation and allows the simulation to be performed on 1 to 2 order magnitudes faster, reaching multi microsecond time scale where more relevant biological phenomenon can be observed. A coarse-grain model of the protein would be useful towards understanding the functional dynamics of the *S. typhi* TolC protein. The gating of TolC has been proposed to involve the twisting of the helices and breaking of intra- and intermonomer hydrogen bond and electrostatic interactions [60, 61]. However, the full dynamics of the protein can only be fully understood in complexation with other accessory proteins, which form the working efflux pump. Coarse-grain simulations have been applied to the *E. coli* AcrB transporter and suggested that protonation of the drug-bound protomer drives the functional rotation to export the drug [62]. In another study, coarse-grain elastic normal-mode analysis has been applied to a model of AcrAB-TolC assembled by molecular docking, revealing concerted motions not only at the contact interface of the individual components but also between distant parts of the entire complex [63]. It would also be interesting to see how the protein functions with other transporters such as MacAB. The use of coarse-grain simulation has also been expanded to lipid bilayer self-assembly on several membrane proteins including *E. coli* TolC, which the authors propose can be used to predict the position of the protein in the membrane [20]. However, as the specific membrane environment could potentially modulate the behavior of some membrane proteins, full detailed atomistic simulation is preferable in many cases [64].

A reliable model of the *S. typhi* TolC protein in a membrane model will facilitate future analysis of the protein, including transport event of small molecules and peptides across the channel. The transport process has wide implications towards understanding the multidrug efflux function of TolC and its homologues, which contributes to resistance against organic solvent, dyes, detergents, and lipophilic antibiotics such as novobiocin, erythromycin, fusidic acid, and cloxacillin. Using rigid body models, Mishima and colleagues have investigated the insertion and release of a solute into and from a cylindrical vessel, a process that mimics the behavior of TolC and its homologues [65]. They proposed that the insertion/release process can be described by solvent-entropy effect arising from the displacement of solvent molecules [65]. A more realistic view of the transport process can be obtained by evaluating the potential of mean force (PMF) with umbrella sampling and related approaches. This method has been used to evaluate permeation of solutes across protein channels, such as the transport of K^+ ion across the KcsA channel [66, 67].

Future studies may include in-depth analysis of the lipid–protein interaction by probing the hydrogen bonding pattern. Vibrational spectroscopy techniques such as infrared spectroscopy have been applied to study the hydration of small molecules [68]. Hydrogen bonding studies using simulation and vibrational spectroscopy between membrane lipids and the protein [69, 70] and also the lipid headgroups with water [71, 72] showed that lipids not only provide a hydrophobic environment for membrane protein folding but also form hydrogen bonds with protein residues, which stabilize it within the membrane.

As with any simulation study, we should be aware of the limitations of the approach. On the issue of convergence, 5 ns is a short timescale in the biological world; membrane equilibration

may require 20–40 ns of simulation time. However, we draw confidence from prior studies of 5–10 ns timescale that were shown to predict the general dynamics of studied protein [23, 73]. Our subject protein has exhibited structural adaptation to the thinner DMPE membrane as a consequence of hydrophobic mismatch. In this case, POPE could be a more suitable lipid model for extended simulation study. This brings forth the implication for future modeling and design study involving molecular dynamics simulation that a well-matched lipid bilayer can be used to minimize structural rearrangement of the protein.

5 Conclusions

In this study we simulated *S. typhi* TolC protein in both POPE and DMPE. The protein was stably inserted into both membranes, maintaining the lipid component's physical properties as well as the protein's conformation. From the PCA result, we predicted the general dynamics of the protein in a lipid bilayer. The TolC protein showed flexibility in the C-terminal, extracellular loops, and α-helical regions. The slight adaptation of the β-barrel to the lower leaflet of DMPE suggests an effect of hydrophobic matching whereby the protein adapts its structure to match the thinner environment of DMPE compared with that of POPE. In view of the importance of the lipids in modulating the structure of membrane proteins, POPE could potentially be a more suitable model for future simulation of the *S. typhi* TolC protein.

Acknowledgments This work was supported by the Universiti Sains Malaysia RUC Grant [1001/PSKBP/8630014] from Malaysia's Ministry of Education. S. W. Leong would also like to thank MyBrainSc from Malaysia's Ministry of Education for scholarship assistance.

References

1. Khan, K., Ganjewala, D., Rao, K.B.: Recent advancement in typhoid research—a review. Adv. Biotechnol. **74**(4), 35–40 (2008)
2. Crump, J.A., Luby, S.P., Mintz, E.D.: The global burden of typhoid fever. Bull. World Health Organ. **82**(5), 346–353 (2004)
3. Ismail, A., Kader, Z.A., Ong, K.H.: Dot enzyme immunosorbent assay for the serodiagnosis of typhoid fever. Southeast Asian J. Trop. Med. Public Health **22**(4), 563–566 (1991)
4. Ismail, A., Ong, K.H., Kader, Z.A.: Demonstration of an antigenic protein specific for *Salmonella typhi*. Biochem. Biophys. Res. Commun. **181**(1), 301–305 (1991)
5. Choong, Y.S., Lim, T.S., Chew, A.L., Aziah, I., Ismail, A.: Structural and functional studies of a 50-kDa antigenic protein from *Salmonella enterica* serovar Typhi. J. Mol. Graph. Model **29**(6), 834–842 (2011)
6. Federici, L., Du, D., Walas, F., Matsumura, H., Fernandez-Recio, J., McKeegan, K.S., Borges-Walmsley, M.I., Luisi, B.F., Walmsley, A.R.: The crystal structure of the outer membrane protein VceC from the bacterial pathogen *Vibrio cholerae* at 1.8 Å resolution. J. Biol. Chem. **280**(15), 15307–15314 (2005)
7. Akama, H., Kanemaki, M., Yoshimura, M., Tsukihara, T., Kashiwagi, T., Yoneyama, H., Narita, S.-I., Nakagawa, A., Nakae, T.: Crystal structure of the drug discharge outer membrane protein, OprM, of *Pseudomonas aeruginosa*: dual modes of membrane anchoring and occluded cavity end. J. Biol. Chem. **279**(51), 52816–52819 (2004)
8. Koronakis, V., Sharff, A., Koronakis, E., Luisi, B., Hughes, C.: Crystal structure of the bacterial membrane protein TolC central to multidrug efflux and protein export. Nature **405**, 914–919 (2000)
9. Zgurskaya, H.I., Nikaido, H.: Bypassing the periplasm: reconstitution of the AcrAB multidrug efflux pump of *Escherichia coli*. Proc. Natl. Acad. Sci. U.S.A. **96**(13), 7190–7195 (1999)
10. Tikhonova, E.B., Zgurskaya, H.I.: AcrA, AcrB, and TolC of *Escherichia coli* form a stable intermembrane multidrug efflux complex. J. Biol. Chem. **279**(31), 32116–32124 (2004)

11. Kobayashi, K., Tsukagoshi, N., Aono, R.: Suppression of hypersensitivity of *Escherichia coli* acrB mutant to organic solvents by integrational activation of the acrEF operon with the IS1 or IS2 element. J. Bacteriol. **183**(8), 2646–2653 (2001)
12. Nishino, K., Yamaguchi, A.: EvgA of the two-component signal transduction system modulates production of the YhiUV multidrug transporter in *Escherichia coli*. J. Bacteriol. **184**(8), 2319–2323 (2002)
13. Borges-Walmsley, M.I., Beauchamp, J., Kelly, S.M., Jumel, K., Candlish, D., Harding, S.E., Price, N.C., Walmsley, A.R.: Identification of oligomerization and drug-binding domains of the membrane fusion protein EmrA. J. Biol. Chem. **278**(15), 12903–12912 (2003)
14. Tanabe, H., Yamasaki, K., Furue, M., Yamamoto, K., Katoh, A., Yamamoto, M., Yoshioka, S., Tagami, H., Aiba, H., Utsumi, R.: Growth phase-dependent transcription of emrKY, a homolog of multidrug efflux emrAB genes of *Escherichia coli*, is induced by tetracycline. J. Gen. Appl. Microbiol. **43**(5), 257–263 (1997)
15. Nagakubo, S., Nishino, K., Hirata, T., Yamaguchi, A.: The putative response regulator BaeR stimulates multidrug resistance of *Escherichia coli* via a novel multidrug exporter system, MdtABC. J. Bacteriol. **184**(15), 4161–4167 (2002)
16. Kobayashi, N., Nishino, K., Yamaguchi, A.: Novel macrolide-specific ABC-type efflux transporter in *Escherichia coli*. J. Bacteriol. **183**(19), 5639–5644 (2001)
17. Raunest, M., Kandt, C.: Locked on one side only: ground state dynamics of the outer membrane efflux duct TolC. Biochemistry **51**(8), 1719–1729 (2012)
18. Smondyrev, A.M., Voth, G.A.: Molecular dynamics simulation of proton transport through the influenza A virus M2 channel. Biophys. J. **83**(4), 1987–1996 (2002)
19. Zhu, F., Hummer, G.: Pore opening and closing of a pentameric ligand-gated ion channel. Proc. Natl. Acad. Sci. U.S.A. **107**(46), 19814–19819 (2010)
20. Scott, K.A., Bond, P.J., Ivetac, A., Chetwynd, A.P., Khalid, S., Sansom, M.S.P.: Coarse-grained MD simulations of membrane protein-bilayer self-assembly. Structure **16**(4), 621–630 (2008)
21. Saito, H., Mizukami, T., Kawamoto, S., Miyakawa, T., Iwayama, M., Takasu, M., Nagao, H.: Molecular dynamics studies of lipid bilayer with gramicidin A: effects of gramicidin A on membrane structure and hydrophobic match. Int. J. Quantum Chem. **112**(2012), 161–170 (2011)
22. Elliott, J.R., Needham, D., Dilger, J.P., Haydon, D.A.: The effects of bilayer thickness and tension on gramicidin single-channel lifetime. Biochim. Biophys. Acta. Biomembr. **735**(1), 95–103 (1983)
23. Debret, G., Valadié, H., Stadler, A.M., Etchebest, C.: New insights of membrane environment effects on MscL channel mechanics from theoretical approaches. Proteins **71**(3), 1183–1196 (2008)
24. Elmore, D.E., Dougherty, D.A.: Investigating lipid composition effects on the mechanosensitive channel of large conductance (MscL) using molecular dynamics simulations. Biophys. J. **85**(3), 1512–1524 (2003)
25. Cordomí, A., Perez, J.J.: Molecular dynamics simulations of rhodopsin in different one-component lipid bilayers. J. Phys. Chem. B. **111**(25), 7052–7063 (2007)
26. Cox, K., Sansom, M.S.: One membrane protein, two structures and six environments: a comparative molecular dynamics simulation study of the bacterial outer membrane protein PagP. Mol. Membr. Biol. **26**(4), 205–214 (2009)
27. Harroun, T.A., Heller, W.T., Weiss, T.M., Yang, L., Huang, H.W.: Experimental evidence for hydrophobic matching and membrane-mediated interactions in lipid bilayers containing gramicidin. Biophys. J. **76**(2), 937–945 (1999)
28. van Meer, G., Voelker, D.R., Feigenson, G.W.: Membrane lipids: where they are and how they behave. Nat. Rev. Mol. Cell. Biol. **9**(2), 112–124 (2008)
29. Tieleman, D.P., Berendsen, H.J.C.: A molecular dynamics study of the pores formed by *Escherichia coli* OmpF porin in a fully hydrated palmitoyloleoylphosphatidylcholine bilayer. Biophys. J. **74**(6), 2786–2801 (1998)
30. Raetz, C.R.: Enzymology, genetics, and regulation of membrane phospholipid synthesis in *Escherichia coli*. Microbiol. Rev. **42**(3), 614–659 (1978)
31. Ruiz, N., Kahne, D., Silhavy, T.J.: Advances in understanding bacterial outer-membrane biogenesis. Nat. Rev. Microbiol. **4**, 57–66 (2006)
32. Word, J.M., Lovell, S.C., Richardson, J.S., Richardson, D.C.: Asparagine and glutamine: using hydrogen atom contacts in the choice of side-chain amide orientation. J. Mol. Biol. **285**, 1735–1747 (1999)
33. Zhang, L., Hermans, J.: Hydrophilicity of cavities in proteins. Proteins **438**, 433–438 (1996)
34. Jo, S., Lim, J.B., Klauda, J.B., Im, W.: CHARMM-GUI membrane builder for mixed bilayers and its application to yeast membranes. Biophys. J. **97**, 50–58 (2009). doi:10.1016/j.bpj.2009.04.013
35. van der Spoel, D., Lindahl, E., Hess, B., Groenhof, G., Mark, A.E., Berendsen, H.J.C.: GROMACS: fast, flexible, and free. J. Comput. Chem **26**(16), 1701–1718 (2005)
36. Buck, M., Bouguet-Bonnet, S., Pastor, R.W., MacKerell, A.D.: Importance of the CMAP correction to the CHARMM22 protein force field: dynamics of hen lysozyme. Biophys. J. **90**(4), L36–L38 (2006)

37. Mackerell, A.D., Bashford, D., Bellott, M., Dunbrack, R.L., Evanseck, J.D., Field, M.J., Fischer, S., Gao, J., Guo, H., Ha, S., Kuchnir, L., Kuczera, K., Lau, F.T.K., Mattos, C., Michnick, S., Ngo, T., Nguyen, D.T., Prodhom, B., Reiher, W.E., Roux, B., Schlenkrich, M., Smith, J.C., Stote, R., Straub, J., Watanabe, M., Wio, J., Yin, D., Karplus, M.: All-atom empirical potential for molecular modeling and dynamics studies of proteins. J. Phys. Chem. B **102**(18), 3586–3616 (1998)
38. Klauda, J.B., Venable, R.M., Freites, J.A., O'Connor, J.W., Tobias, D.J., Mondragon-Ramirez, C., Vorobyov, I., MacKerell, A.D., Pastor, R.W., Connor, J.W.O.: Update of the CHARMM all-atom additive force field for lipids: validation on six lipid types. J. Phys. Chem. B **114**(23), 7830–7843 (2010)
39. Bussi, G., Donadio, D., Parrinello, M.: Canonical sampling through velocity rescaling. J. Chem. Phys. **126**(1), 014101–014101 (2007)
40. Parrinello, M., Rahman, A.: Polymorphic transitions in single crystals: a new molecular dynamics method. J. Appl. Phys. **52**(12), 7182–7190 (1981)
41. Hoover, W.G.: Canonical dynamics: equilibrium phase-space distributions. Phys. Rev. A **31**(3), 1695–1697 (1985)
42. Nosé, S.: A molecular dynamics method for simulations in the canonical ensemble. Mol. Phys. **52**(2), 255–268 (1984)
43. Hess, B., Bekker, H., Berendsen, H.J.C., Fraaije, J.G.E.M.: LINCS: a linear constraint solver for molecular simulations. J. Comput. Chem. **18**(12), 1463–1472 (1997)
44. Mori, T., Ogushi, F., Sugita, Y.: Analysis of lipid surface area in protein-membrane systems combining Voronoi tessellation and Monte Carlo integration methods. J. Comput. Chem. **33**(3), 286–293 (2012)
45. Jämbeck, J.P.M., Lyubartsev, A.P.: An extension and further validation of an all-atomistic force field for biological membranes. J. Chem. Theory Comput. **8**, 2938–2948 (2012)
46. Rand, R.P., Parsegian, V.A.: Hydration forces between phospholipid bilayers. Biochim. Biophys. Acta. Rev. Biomembr. **988**(3), 351–376 (1989)
47. Rappolt, M., Rapp, G.: Simultaneous small- and wide-angle X-ray diffraction during the main transition of dimyristoylphosphatidylethanolamine. Ber. Bunsenges Phys. Chem. **100**(7), 1153–1162 (1996)
48. Vaccaro, L., Scott, K.A., Sansom, M.S.P.: Gating at both ends and breathing in the middle: conformational dynamics of TolC. Biophys. J. **95**(12), 5681–5691 (2008)
49. Vigh, L., Escriba, P.V., Piotto, S., Maresca, B., Horva, I., Escribá, P.V., Sonnleitner, A., Sonnleitner, M., Horváth, I., Harwood, J.L.: The significance of lipid composition for membrane activity: new concepts and ways of assessing function. Prog. Lipid. Res. **44**(5), 303–344 (2005)
50. Gapsys, V., Groot, B., Briones, R.: Computational analysis of local membrane properties. J. Comput. Aided Mol. Des. **27**(10), 845–858 (2013)
51. Sapay, N., Tieleman, D.P.: Combination of the CHARMM27 force field with united-atom lipid force fields. J. Comput. Chem. **32**(7), 1400–1410 (2011)
52. Jensen, M.Ø., Mouritsen, O.G.: Lipids do influence protein function—the hydrophobic matching hypothesis revisited. Biochim. Biophys. Acta. Biomembr. **1666**, 205–226 (2004)
53. Andersen, O.S., Koeppe, R.E.: Bilayer thickness and membrane protein function: an energetic perspective. Annu. Rev. Biophys. Biomol. Struct. **36**, 107–130 (2007)
54. Kandasamy, S.K., Larson, R.G.: Molecular dynamics simulations of model trans-membrane peptides in lipid bilayers: a systematic investigation of hydrophobic mismatch. Biophys. J. **90**(7), 2326–2343 (2006)
55. Venturoli, M., Smit, B., Maddalena, M., Sperotto, M.M.: Simulation studies of protein-induced bilayer deformations, and lipid-induced protein tilting, on a mesoscopic model for lipid bilayers with embedded proteins. Biophys. J. **88**(3), 1778–1798 (2005)
56. Wang, Y., Schlamadinger, D.E., Kim, J.E., McCammon, J.A.: Comparative molecular dynamics simulations of the antimicrobial peptide CM15 in model lipid bilayers. Biochim. Biophys. Acta. Biomembr. **1818**(5), 1402–1409 (2012)
57. Lins, R.D., Straatsma, T.P.: Computer simulation of the rough lipopolysaccharide membrane of *Pseudomonas aeruginosa*. Biophys. J. **81**(2), 1037–1046 (2001)
58. Piggot, T.J., Holdbrook, D.A., Khalid, S.: Electroporation of the *E. coli* and *S. aureus* membranes: molecular dynamics simulations of complex bacterial membranes. J. Phys. Chem. B **115**, 13381–13388 (2011)
59. Nikaido, H.: Molecular basis of bacterial outer membrane permeability revisited. Microbiol. Mol. Biol. Rev. **67**(4), 593–656 (2003)
60. Andersen, C., Koronakis, E., Bokma, E., Eswaran, J., Humphreys, D., Hughes, C., Koronakis, V.: Transition to the open state of the TolC periplasmic tunnel entrance. Proc. Natl. Acad. Sci. U.S.A. **99**(17), 11103–11108 (2002)
61. Eswaran, J., Hughes, C., Koronakis, V.: Locking TolC entrance helices to prevent protein translocation by the bacterial type I export apparatus. J. Mol. Biol. **327**(2), 309–315 (2003)
62. Yao, X.-Q., Kenzaki, H., Murakami, S., Takada, S.: Drug export and allosteric coupling in a multidrug transporter revealed by molecular simulations. Nat. Commun. **1**, 117 (2010)

63. Wang, B., Weng, J., Fan, K., Wang, W.: Elastic network model-based normal mode analysis reveals the conformational couplings in the tripartite AcrAB-TolC multidrug efflux complex. Proteins **79**(10), 2936–2945 (2011)
64. Ash, W.L., Zlomislic, M.R., Oloo, E.O., Tieleman, D.P.: Computer simulations of membrane proteins. Biochim. Biophys. Acta. Biomembr. **1666**, 158–189 (2004)
65. Mishima, H., Oshima, H., Yasuda, S., Amano, K.-I., Kinoshita, M.: Entropic release of a big sphere from a cylindrical vessel. Chem. Phys. Lett. **561**, 159–165 (2013)
66. Burykin, A., Schutz, C.N., Villá, J., Warshel, A.: Simulations of ion current in realistic models of ion channels: the KcsA potassium channel. Proteins **47**(3), 265–280 (2002)
67. Burykin, A., Kato, M., Warshel, A.: Exploring the origin of the ion selectivity of the KcsA potassium channel. Proteins **52**(3), 412–426 (2003). doi:10.1002/prot.10455
68. Stare, J., Mavri, J., Grdadolnik, J.E., Zidar, J., Maksić, Z.B., Vianello, R.: Hydrogen bond dynamics of histamine monocation in aqueous solution: Car–Parrinello molecular dynamics and vibrational spectroscopy study. J. Phys. Chem. B **115**(19), 5999–6010 (2011)
69. Deol, S.S., Bond, P.J., Domene, C., Sansom, M.S.P.: Lipid-protein interactions of integral membrane proteins: a comparative simulation study. Biophys. J. **87**(6), 3737–3749 (2004)
70. Sanchez, K.M., Kang, G., Wu, B., Kim, J.E.: Tryptophan-lipid interactions in membrane protein folding probed by ultraviolet resonance Raman and fluorescence spectroscopy. Biophys. J. **100**(9), 2121–2130 (2011)
71. Zhao, W., Moilanen, D.E., Fenn, E.E., Fayer, M.D.: Water at the surfaces of aligned phospholipid multibilayer model membranes probed with ultrafast vibrational spectroscopy. J. Am. Chem. Soc. **130**(42), 13927–13937 (2008)
72. Nagata, Y., Mukamel, S.: Vibrational sum-frequency generation spectroscopy at the water/lipid interface: molecular dynamics simulation study. J. Am. Chem. Soc. **132**(18), 6434–6442 (2010)
73. Straatsma, T.P., Soares, T.A.: Characterization of the outer membrane protein OprF of *Pseudomonas aeruginosa* in a lipopolysaccharide membrane by computer simulation. Proteins **74**, 475–488 (2009)